MADRID
inter.noise 2019
June 16 - 19
NOISE CONTROL FOR A BETTER ENVIRONMENT

Experiment and simulation of influence of distorted inlet flow on aerodynamic noise in small axial fan

Ryuta Shinohara [1]
Gaku Minorikawa[1]
Takefumi Nakano[1]
Ryoichi Maki[1]
Course of Mechanical Engineering, Graduate school of Hosei University
3-7-2, Kajinocho, Koganei-shi, Tokyo, 184-8584, Japan

Tae-Gyun Lim[2]
CEDIC Co. Ltd., Seoul, Korea

ABSTRACT

The present study is concerning about experiment and simulation of generation mechanism and prediction of aerodynamic noise from small axial fan for information technology devices at distorted inlet flow operation. Small fan tends to place at narrow and small space, inlet flow becomes asymmetric due to obstacles and separated flow increases aerodynamic noise. In the study, a small asymmetric obstacle was set at the casing inlet of an axial small fan with 166mm impeller diameter, the effect on noise was measured and the aerodynamic noise was calculated by CFD and CAA simulation. In addition, the distribution of the aerodynamic noise source was examined by measuring the pressure fluctuation on the casing surface.

Keywords: Small axial fan, Aerodynamic noise, Pressure fluctuation, Asymmetric Obstacle, Casing inlet shape
I-INCE Classification of Subject Number: 10

[1] ryuta.shinohara.6j@stu.hosei.ac.jp
[1] minori@hosei.ac.jp
[1] takefumi.nakano.8z@stu.hosei.ac.jp
[1] ryouichi.maki.2x@stu.hosei.ac.jp
[2] tglim@cedic.biz

1. INTRODUCTION

In recent years, as explosive demands of internet, large scale data centers are constructing worldwide. In the data center, there are number of server machines that generate huge amount of heat. So, there are so many cooling fans, the noise is serious problem which sound pressure level so large. In some cases, the cooling axial fan is inevitably installed in a narrow space or with an obstacle, the flow channel is distorted asymmetrically and the aerodynamic noise increases. In this research, in order to evaluate the influence of the inlet shape of the casing and the inlet obstacle on the aerodynamic noise in a small axial flow fan, characteristics of pressure fluctuation on the casing surface as one of aerodynamic noise sources were evaluated by experiment and numerical simulation (CFD).

2. FAN NOISE

In general, it is said that the aerodynamic noise generated from axial fan is roughly divided into the rotating and the turbulent flow. At first, due to the blades passing of the impeller, the rotating noise is produced by the periodic pressure fluctuations. The rotating noise has the discrete components at the Blade Passing Frequency (BPF) which is the product of the number of blades Z [-] and rotating speed n [rps] and its harmonics. It is the large contribution to the overalls of the fan noise. On the other hand, the turbulent noise is caused by the random flow in the fan. It is known that the pressure fluctuations on the surface of the impeller and of the casing presents the noise source. The turbulent noise generally distributes in broadband frequency and the contribution to the overall sound pressure level is less than the rotating noise normally.

3. EXPERIENTAL SETUP

3.1 Experimental Apparatus

As shown in the Figure 1, the tested fan was the axial flow fan with 5 blades impeller, outside diameter D_2=166 mm and the casing with 4 spokes and inlet flange width W=14.5 mm. It was driven by an AC motor and operated at N=2850 rpm. The impeller and fan casing were fabricated by stereo lithography with the additive layer pitch by 0.1 mm.

Figure 2 shows the casings having various inlet corner shape. The original casing had the flange with the right angle to the casing. The modified casings had the round shape that the Case1 was the curvature radius by the flange width, the Case2 was the same radius as the Case1 with the half-length of the Case1 and the Case3 was half circle with the diameter by the flange width. These were designed to eliminate the flow separation at the edge and reduce the turbulent noise.

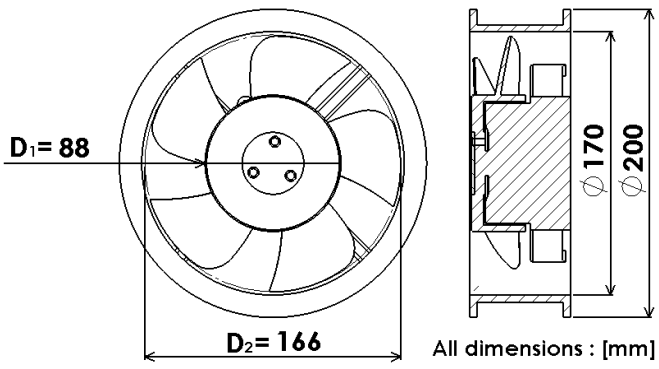

Fig.1 – Front view of tested fan

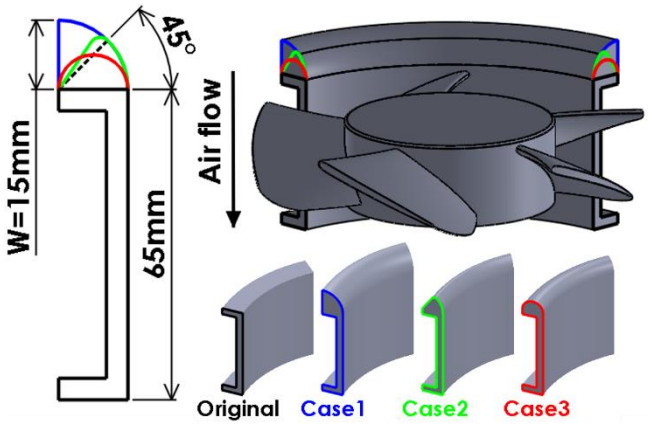

Fig.2– Inlet corner shape of casing

3.2 Inlet Obstacle

A thick rectangular plate shown in Figure 3 was installed as an inlet obstacle on the fan suction side. As can be seen from the right side of Figure 3, the inner distance between the surface of the casing and the obstacle was defined as "G", in which the total length in the fan axial direction was equal and the value was set by 20, 30 and 40 mm. So, the actual distance from obstacle to casing surface was different for each casing.

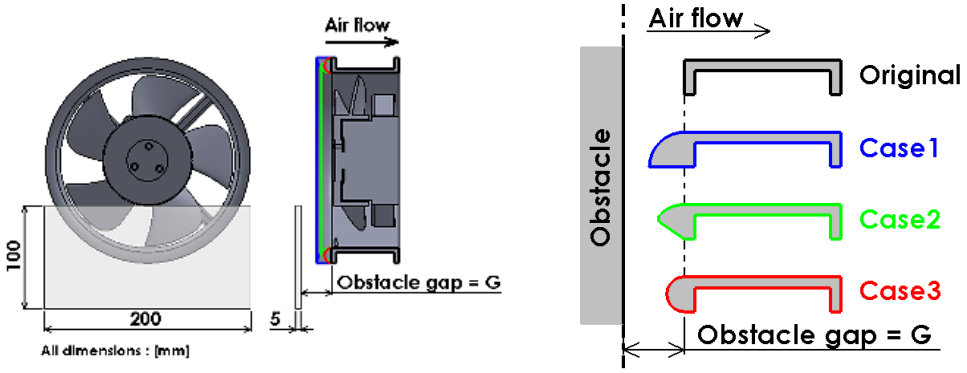

Fig.3– Position of inlet obstacle

3.3 Setup for Fan Noise Measurement

Figure 4 shows the noise measurement setup of the tested fan. The noise was measured in a hemi-anechoic room which room size was 2.8 m in width, 2.8 m in length and 3.1 m in height. The fan was suspended by stringers without the flow restriction to the external environment. In general, the fan is operated at a determined operating point with a duct which produces a pressure difference between the suction side and discharge side, but in this study, the adverse effects such as the acoustic frequency characteristics and the radiated sound due to the vibration of the duct were excluded to observe the emitted fan noise clearly. A sound level meter was set at the position, where 1 m away from the fan inlet surface, on the axis of 80 degrees from the axial direction. The noise signal was measured for 10 seconds and analyzed in the band up to 5000Hz by FFT analyzer.

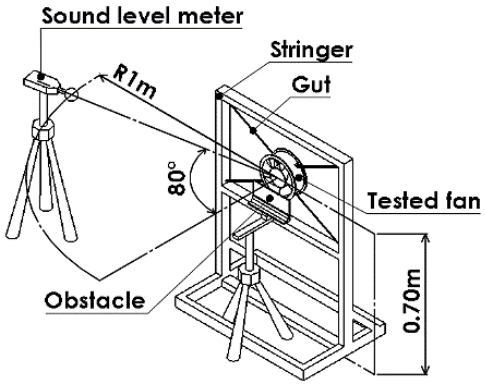

Fig.4– Measurement setup of fan noise

3.4 Measurement Setup of Pressure Fluctuation on Casing Surface

Figure 5 shows the positions of the pressure taps to measure the pressure fluctuation on the casing surface. There are 5 ports along circumferential direction around the inlet corner and another 5 ports along mainstream direction, denoted as P1a to P1e and P1 to P5, respectively.

Figure 6 shows the arrangement of the MEMS microphones. The microphone was 4 mm width, 6 mm length and 1.5 mm diameter of the sensing hole with flat frequency response from 100 Hz to 5 kHz. In order to avoid the effect of steady static pressure, the sensing hole was covered by an acoustically transparent film. The calibration of MEMS microphone was performed by the sound calibrator (RION NC-75) with the film. The signal recording and frequency analysis were done at the same time with the noise measurement.

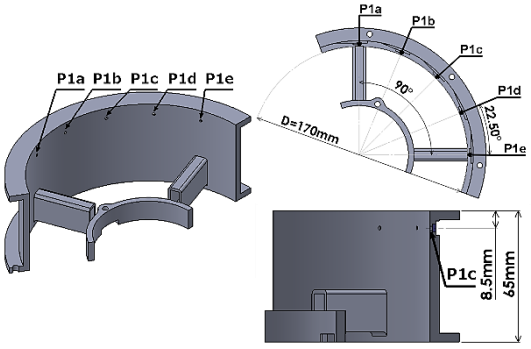

Fig.5– Pressure fluctuation ports on the casing surface

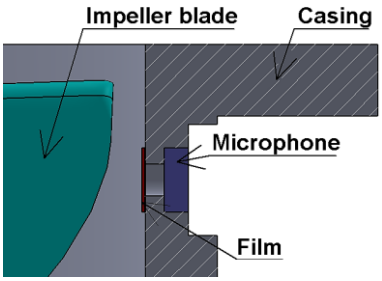

Fig.6– Cross sectional view of pressure holes on casing

4. SIMULATION SETUP

The numerical simulation was carried out by using commercial software (Cradle SCRYU/Tetra) which is using unconstructed grid system based on Navier-Stokes

equation. In order to evaluate the inlet shape and the influence of the inlet obstacle on the flow near the wall surface, The calculation model simulating a free air condition except the inlet obstacle was made. It consists of an sphere around the fan, a impeller, a casing and an inlet obstacle as shown in Figure 7. The diameter of the sphere was 11 times the outer diameter of the casing. The number of mesh elements was totally about 9,000,000 that consists of the impeller circumference, the casing and the obstacle, and the surrounding air region by 4.4 million, 3.5 million and 1.1 million, respectively. The zero total pressure was set as the inlet condition and all solid bodies were defined as stationary walls. The ALE method was used to reproduce the rotation of the fan and the impeller surface was made to rotate moving wall which rotating speed was set to 2850 rpm. After performing a steady state analysis with governing equation RANS and turbulence model SST k - ω for 200 cycles, the result was applied as an initial value for unsteady LES calculation and the time required for the fan to rotate by about 4 revolutions, in which the time interval was 1/17100 seconds.

The influence of the inlet shape and the inlet obstacle was evaluated by comparing the flow velocity distribution and static pressure distribution of meridional section as shown in Figure 8.

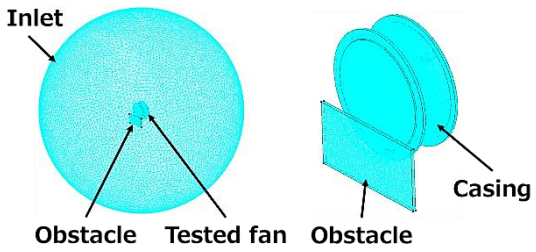

Fig.7– Numrical simulation model

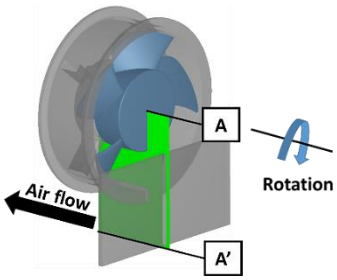

Fig.8– Position of meridian cross section A-A'

5. RESULT AND DISCUSSIONS

5.1 Noise characteristics

5.1.1 Influence of inlet obstacle

Figure 9 shows a comparison of the fan radiated sound spectrum when the distance of the obstacle was changed. In the frequency up to 2000 Hz, not only the blade passing frequency and its harmonics but also the turbulent noise components increased when the distance of the obstacle was shorter. On the other hand, the influence on the turbulent noise in the 3000 to 5000 Hz band was small. This tendency was confirmed also in Case2 and Case3.

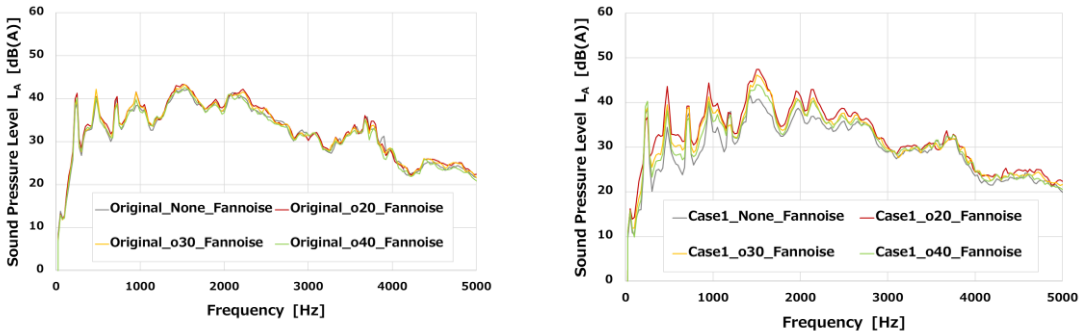

Original *Case1*

Fig.9– Radiated fan noise spectra
(Comparison of obstacle gap: G)

5.1.2 Influence of inlet shape

Figure 10 shows the comparison of noise when the casing inlet shape was changed. It was confirmed that the sound pressure level was reduced due to the change of the inlet shape at at 570 Hz, which is second harmonics of the BPF, and the sound pressure level decreased in the broadband frequency up to 2000 Hz. By changing the shape of the inlet, not only the BPF noise due to the interference between the impeller and but also the broadband noise due to the separation up to 2000 Hz were reduced. On the other hand, in the frequency band over 2000 Hz, the sound pressure level was not decreased by the modified casing. Totally speaking, it is said that the best shape for the noise reduction was the Case3, which clearance was the largest.

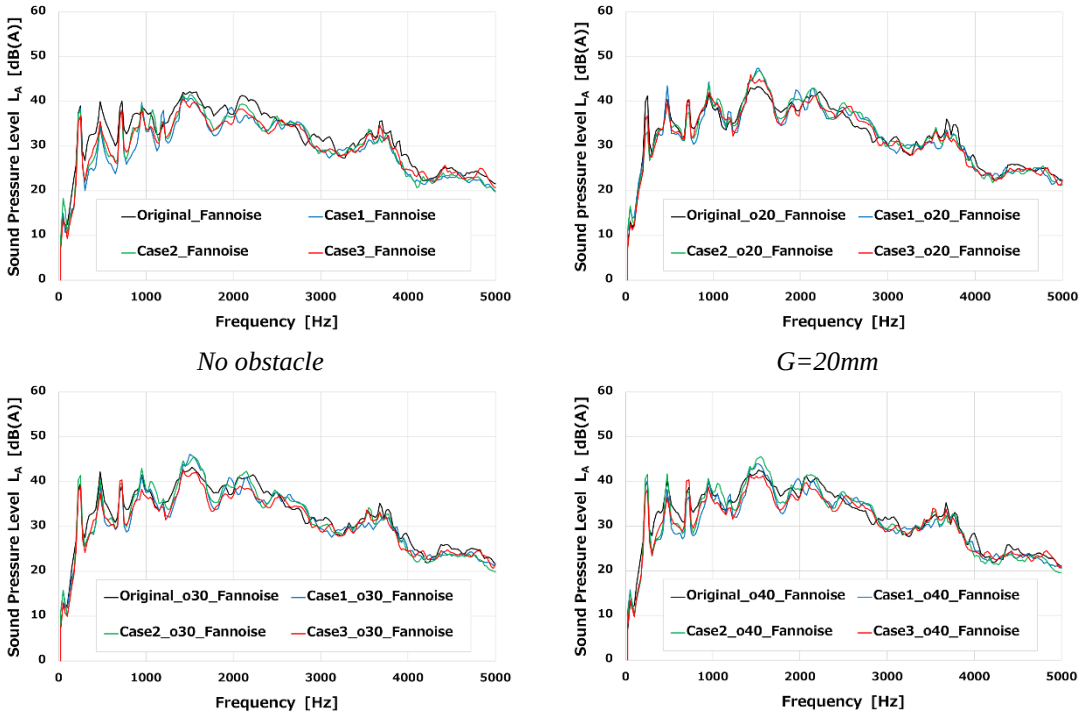

No obstacle *G=20mm*

G=30mm *G=40mm*

Fig.10– Radiated fan noise spectra
(Comparison of shape of casing)

5.2 Result of pressure Fluctuations

5.2.1 Influence of inlet obstacle

Figure 11 shows the relationship between the obstacle distance and the pressure fluctuation level on the pressure hole. The closer the distance of the obstacle was, the more the BPF and its harmonic components increased. Moreover, in the broadband from 500 to 5000 Hz, the level increased as the distance of the obstacle got closer. A similar tendency was seen in the Case2 and Case3.

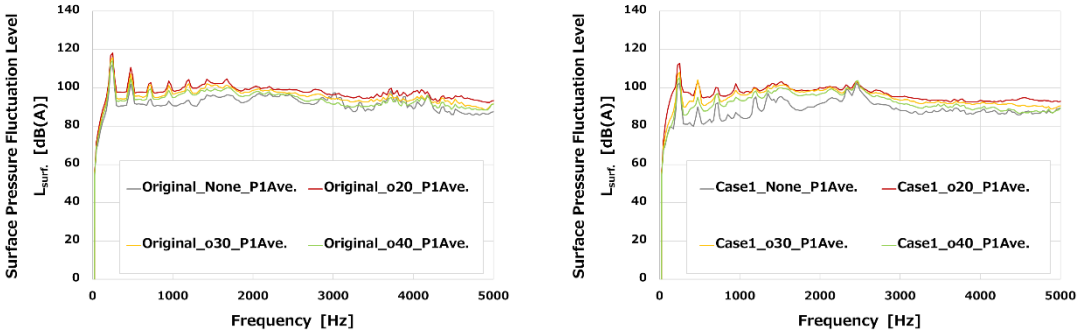

Original *Case1*

Fig.11– Pressure fluctuation spectra on casing edge (Comparison of obstacle gap: G)

5.2.2 Influence of inlet shape

Figure 12 shows the relationship between the inlet shape and the pressure fluctuation level on the pressure hole. By the casing roundness, the level was reduced in the BPF and in the broadband up to 2000 Hz, which was the same trend as the radiated noise. Comparing the level between BPF and the broadband noise, the former one was higher by 10dB. It can be said that the main factor of the pressure fluctuation on the casing wall surface was derived from the blade passage. The harmonic components of BPF also appeared, however, these levels were smaller than the 1st BPF level while those in the radiated noise were almost equal. In addition, the broadband noise level in the Case1 was relatively smaller than the other casings in spite of the narrowest clearance.

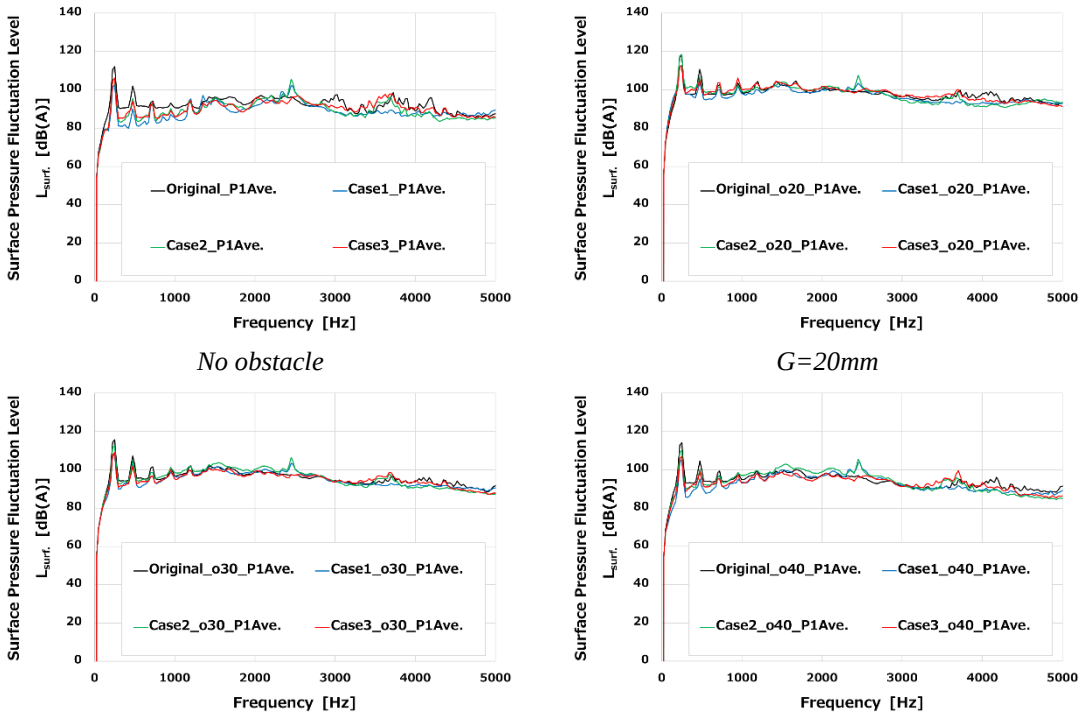

No obstacle *G=20mm*

G=30mm *G=40mm*

Fig.12– Pressure fluctuation spectra on casing edge (Comparison of shape of casing)

5.3 Result of simulation

5.3.1 Influence of inlet obstacle

Figure 13 and Figure 14 show the simulation results of the instantaneous flow velocity distributions of the Original and the Case1 with G = 20 mm in the blade meridional section A - A', especially around the inlet obstacle. In the case of the Original, the inlet flow came from not only the axial opening but also the clearance between the obstacle and the casing edge in the radial direction. In the Case1, as the clearance was smaller, the inlet flow velocity from the axial opening was larger and the flow in the radial direction was faster due to small clearance. It is said that the inlet flow around the obstacle was strongly affected by the clearance and these unsteady changes of the flow could be related to the noise source.

The static pressure distributions of the Original and the Case1 are shown in Figure 15 and Figure 16. In case of the Original, the low pressure region was found around the upper side of the blade and the casing edge. On the other hand, the Case1 showed wider low pressure region around the clearance between the obstacle and the casing. The tendency matches that of the flow velocity distributions. Furthermore, the trends of instantaneous pressure on the casing surface in the Original and the Case1 were different, so it is also said the change of the clearance affected the noise source characteristics.

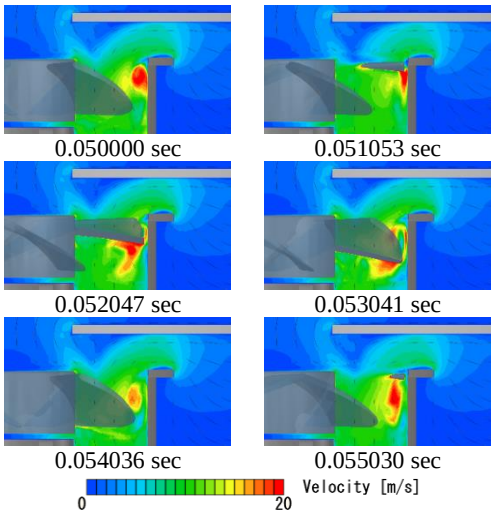

Fig.13– Velocity contour on cross section A-A' (Casing:Original, Obstacle gap: G=20mm)

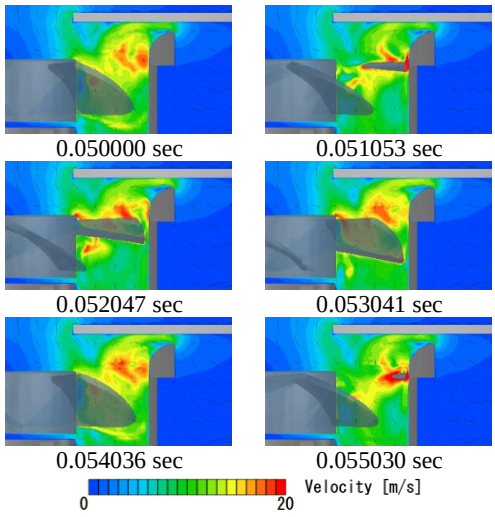

Fig.14– Velocity contour on cross section A-A' (Casing:Case1, Obstacle gap: G=20mm)

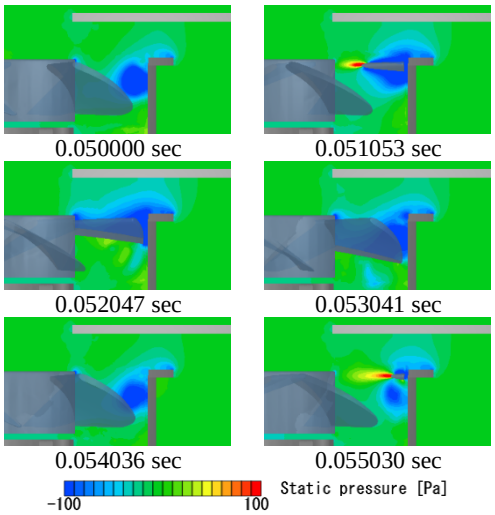

Fig.15– Static pressure contour on cross section A-A' (Casing:Original, Obstacle gap: G=20mm)

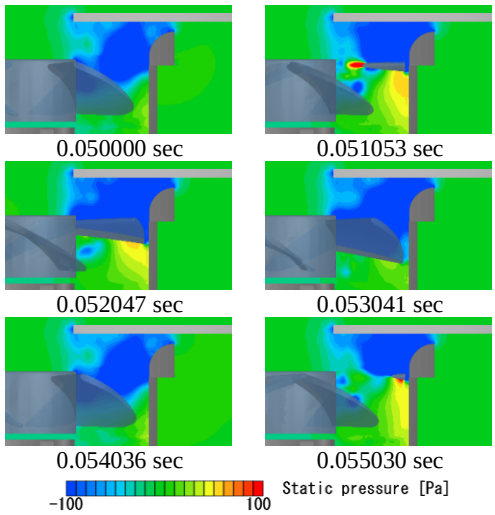

Fig.16– Static pressure contour on cross section A-A' (Casing:Case1, Obstacle gap: G=20mm)

5.3.2 Influence of inlet shape without inlet obstacle

The flow velocity distributions of the Original and the Case1 without the obstacle in meridional section A - A' and these static pressure distributions are shown in Figure 17, Figure 18, Figure 19 and Figure 20, respectively. As shown in Figure 17 and Figure 18, the inlet flow acceralated rapidly at the casing edge. In the case of the Original which casing edge was close to the blade, high velocity region looking like strong vortex was found around the blade tip. On the other hand, the inlet flow of the Case1 gradually acceralated from casing edge and there was no strong vortex. As well as the pressure distributions shown in Figure 19 and Figure 20, a local low pressure region around the blade tip was found in the Original and the Case1 and the scale of the Case1 was smaller. It is clear that the modified casing shape improved the inlet flow conditon witout the obstacle.

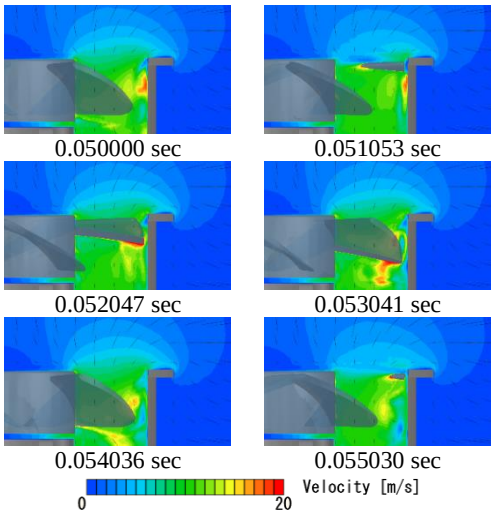

Fig.17– Velocity contour on cross section A-A'
(Casing: Original, No obstacle)

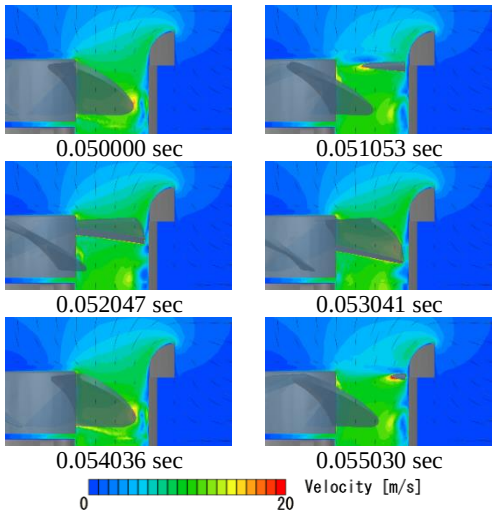

Fig.18– Velocity contour on cross section A-A'
(Casing:Case1, No obstacle)

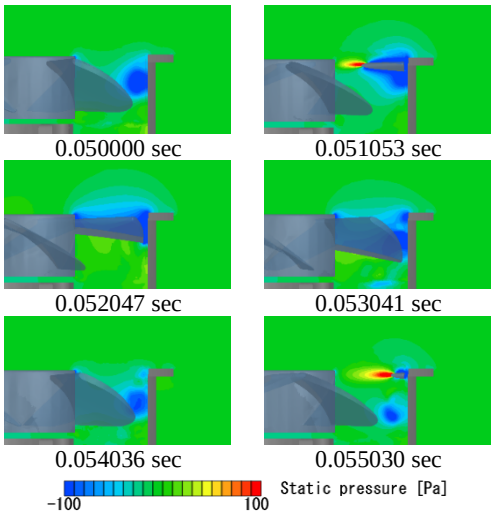

Fig.19– Static pressure contour on cross section A-A'
(Casing:Original, No obstacle)

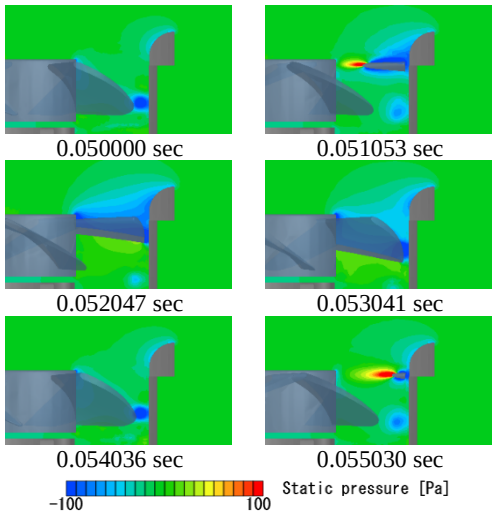

Fig.20– Static pressure contour on cross section A-A'
(Casing:Case1, No obstacle)

6. SUMMARY

For noise reduction of a small axial fan with an asymmetric inlet obstacle, the influence of the casing inlet shape on the noise and the pressure fluctuation of the casing wall surface related to aerodynamic noise source was evaluated by experiment and simulation. The inlet obstacle increased the noise and the pressure fluctuation on the casing wall near the inlet. By changing the casing inlet shape, the pressure fluctuations at BPF components could be reduced and there was little effect to reduce random fluctuations distributed in the broadband from 2000 to 5000 Hz. It was cleared that the casing inlet shape and the clearance between the obstacle and the casing edge were strongly affected the flow distribution behind the obstacle by simulation.

7. REFERENCES

1. Gaku Minorikawa, Wan-Ho Jeon, Tae-Gyun Lim and Hyon-gi Hon, “Prediction and Identification of the Aerodynamic Noise Source on Small Axial Fan”, Noise-Con 2014, NC14_126 (2014)
2. Gaku Minorikawa, Tae-Gyun Lim and Wan-Ho Joen, “Prediction for Noise Reduction and Characteristics of Flow-Induced Noise on Axial Cooling Fan”, 24th International Congress on Sound and Vibration, 2329-3675 (2017)
3. Ryouichi Maki, Gaku Minorikawa, Takefumi Nakno and Tae-Gyun Lim, “Study on Identification and Reduction of Aerodynamic Noise Source on Casing in Axial Flow Fan”, Proceedings of Inter-Noise2018, No.1626 (2018)